Deformation field in indentation of a granular ensemble

Tejas G. Murthy, Ebenezer Gnanamanickam, and Srinivasan Chandrasekar

Phys. Rev. E **85**, 061306 — Published 14 June 2012

DOI: 10.1103/PhysRevE.85.061306

Deformation field in indentation of a granular ensemble

Tejas G Murthy[*]

[*]*Indian Institute of Science, Bangalore, India.*

Ebenezer Gnanamanickam[+] and Srinivasan Chandrasekar[+]

[+]*Purdue University, West Lafayette, IN, USA*

An experimental study has been made of the flow field in indentation of a model granular material. A granular ensemble composed of spherical sand particles with average size of 0.4 mm is indented with a flat ended punch under plane-strain conditions. The region around the indenter is imaged *in situ* using a high-speed Charge-Coupled Device (CCD) imaging system. By applying a hybrid image analysis technique to image sequences of the indentation, flow parameters such as velocity, velocity gradient and strain rate are measured at high resolution. The measurements have enabled characterization of the main features of the flow such as dead material zones, velocity jumps, localization of deformation, and regions of highly rotational flow resembling vortices. Implications for validation of theoretical analyses and applications are discussed.

I. INTRODUCTION

Granular materials occupy a unique space between solids and fluids and this behavior is manifested at multiple length scales. The forces applied on the boundary of a granular medium are transmitted between the grains via their contacts through the formation of structural entities referred to as force chains. These chains have a characteristic length scale which is generally greater than the mean particle size, implying that the transmission of forces is heterogeneous[1]. The force transmission leads to substantial deformation manifesting at various length scales.

Consequently, the deformation in granular materials at an ensemble level is heterogeneous and anisotropic, characterized by strain localization and shear banding. At the particle level too, this

deformation is characteristically non homogeneous [2]. In contrast to metals, the deformation in granular ensembles is non affine with considerable local fluctuations in the velocity and rotation of the particles[2](Affine deformation is defined as that type of deformation in which the gradients in the kinematical properties of two adjacent particles can be reasonably represented by their mean gradients). Experiments have suggested a significant deviation in the principal axes of stress and strain-increments indicating substantial non-associativity in the flow rules of granular materials. The kinematics of flow, friction and transmission of forces is critical to understanding mechanical behavior; deformation processing by processes such as rolling, forging and extrusion, impinging on applications in pharmaceuticals [3], powder metallurgy[4, 5] and ceramics processing[6], motion of objects through granular ensembles[7] and design of structural foundations [8]

With this as background, an experimental study has been made of flow and deformation in granular materials. The model experimental system studied is slow shearing of a granular ensemble by plane strain indentation with a flat ended punch. The flow is characterized at micrometer-level resolution using high-speed imaging and image correlation techniques that can handle both steady and non-steady deformation. Special attention is paid to characterizing jumps and fluctuations in velocity at a mesoscale, and to flow characteristics such as stagnation and rotation. Besides its intrinsic value for exploring and discriminating theoretical models of deformation and flow of granular ensembles, this model system has direct relevance to applications ranging from motion of objects in sand to deformation processing of granular solids into bulk forms. The relation between punch indentation and deformation processing is well known from prior studies on metals [5,9].

II. BACKGROUND

Optical and image based experiments with model granular materials have contributed significantly to current understanding of the flow behavior of these materials. The force chain network has been visualized and characterized through photoelasticity, wherein assemblages of photoelastic disks simulating the granular medium were imaged under different boundary conditions. The propagation of stresses in the medium was visualized through birefringence[10].

The photoelasticity experiments have paved the way for reliable estimates of contact forces between the particles and, by extension, their transmission from the loading zone to the boundary of the object under study. In another photoelastic study, the displacements of particles were traced in a 2D Couette cell; this exercise also highlighted the deformation within a shear band[11]. Local fluctuations of individual particle displacements were found to be dominant and discernable even at low strains, while also influencing the ensemble behavior. The experiments showed a comparable scale effect on affine (elastic) deformations and non-affine plastic deformations, i.e. the affine and non-affine deformations appeared to contribute equally to the deformation in a granular ensemble.

Features such as shear bands often occur in deformation and flow of granular media. These shear bands represent "discontinuities" or rapid jumps in velocity; the velocity discontinuities correspond to localization of strain [7, 12]. Schall and Van Hecke [12] have provided a review of shear bands in many types of granular media along with specific characteristics and the principal mechanisms underlying their formation at the continuum scale. The shear band size was found to show specific scaling characteristics with respect to particle size in sand. However, no strong correlation between stress features such as force chains and deformation features like shear bands could be established.

Numerical methods, especially DEM simulations, have been used in parallel with experiments to probe propagation of force chains at multiple temporal and spatial scales and to understand the flow behavior of the ensembles. Quantitative algorithms for characterizing force chains at the mesoscale from DEM simulations have been reported based on microlevel descriptions of inter-particle contact friction, packing density and degree of polydispersity [13]. DEM simulation has also been used to explore similarities between the force chain network and the relative displacement of the granular material under quasistatic deformation conditions [14]. Akin to the well known strong and weak force chain networks, analogous networks based on deformation were identified, viz. mobile and immobile networks. A strong decoupling between the mobile and the strong network was noted, confirming lack of strong correlation between the recorded forces and displacements. These observations are in agreement with some experiments that investigated flow rules [15], albeit in the framework of the mathematical theory of plasticity, using optically sensitive glass particles.

The quasistatic indentation of a granular ensemble by a flat punch considered in this study offers a clean experimental system for studying flow, deformation and friction in this class of materials, based on prior studies with metals. This system, which involves non-steady and non self-similar flow, can also be considered as the slow flow of a granular material around a rigid object or obstacle. A well-known application of this problem is in design of foundations for buildings. The classical treatments of this problem are based on Prandtl's pioneering analysis of flat punch indentation of metals[9]. The resistance of the granular ensemble to the penetration of the indenter is a measure of the strength of the ensemble. A body of literature exists wherein this load bearing capacity has been examined through finite element and discrete element methods, limit analysis methods from the theory of plasticity and different types of experiments. An early experimental study of this problem involved imaging of sand trajectories using markers in select regions under model indenters [16]. More recently, displacements and strains in punch indentation of sand have been estimated through particle image velocimetry (PIV) [17,18, 19]. Another somewhat related problem that has been explored by image analysis is motion of a "finger" through a granular ensemble [20]. Image analysis details in the latter study are somewhat sparsely described and the configuration of a moving indenter used therein is not amenable to continuous characterization of velocities and deformation associated with the flow. A diffuse wave spectroscopic technique has also been used to spatially image the deformation field in gelatin [21]. Even with these experimental advancements, accurate assessment of the deformation field at multiple length scales is challenging due to inherent inaccuracies in a correlation based method such as PIV [22] and the short length scales in photoelasticity experiments. Specifically, measurement of velocity, strain rate, and strain in highly localized regions such as indenter-ensemble interfaces, indenter walls and shear bands has posed difficulties.

The present study combines high-speed imaging and multiple (complementary) feature tracking techniques to characterize the flow in punch indentation at high resolution. A hybrid extension of the PIV employing particle tracking and optical flow algorithms, applied originally to analyze indentation and cutting of metals [23, 24] and in a preliminary study of granular ensembles [19], is seen to play a key role in the mesoscale characterization of flow.

III. EXPERIMENTAL

The deformation and flow of a model granular medium – quartzite sand – at small deformation rates was studied using plane-strain (2D) punch indentation. Figure 1 shows a schematic and detailsof the experimental arrangement. The quartzite sand grains were of mean grain diameter (d), 0.4mm, and variance of about 0.07mm, this tight distribution of grain size assuring a nearly mono-disperse medium. The grains were confined in chamber made of Perspex 750 mm X 450 mm X 150 mm, and indented with a flat-ended steel punch of size 45 mm X 150 mm X 150 mm on a universal testing machine (UTM). The half-width of the punch is defined as 'a'; this dimension is used to normalize length parameters when presenting results pertaining to the flow field. These dimensions are typically sufficient to ensure plane strain conditions based on prior work [16-19].

A medium dense packing configuration of the sand (relative density of 65-70%) was used. This relative density is the ratio of the difference in the maximum and current void ratio to the maximum and minimum void ratios. This packing density was achieved by controlling the drop height of the sand into the chamber and gently tapping the sides of the box. The Perspex chamber was placed on the bottom (movable) platen of the testing machine while the indenter was attached to the top (fixed) platen. The chamber could be moved at speeds of up to 50 mm/s enabling various deformation rates and studies of the rate sensitivity of granular materials to indentation.

The flow of the material during indentation was imaged at high resolution using a high-speed CCD camera (PCO 1600, Cooke Corp.). A monochromatic light source was used to illuminate the region of interest around the indenter. The inherent texture in the sand produces a speckle pattern under lighting; this provides high-quality markers for the image analysis to characterize the deformation. A novel aspect of the experimental arrangement (Fig. 1) is that the sand-filled chamber traverses the field of view of the camera, which remains fixed with respect to the indentation region, enabling continuous tracking of the flow. Such tracking is difficult to realize in the commonly used indentation set-ups that employ a moving indenter [20]. The indentation speed used in the experiments was 1.5mm/min (~0.026mm/s). During the indentation, a region of ~ 145mm X 110mm around the indenter was imaged *insitu* at 0.25 fps. The typical per pixel spatial resolution was 0.008 mm. This arrangement thus provided a good compromise between

imaging sufficiently large areas so as to capture the flow field and capturing microscopic aspects of the flow. In a few experiments, a smaller field of view was used to achieve higher magnification of the flow.

The distance of penetration of the indenter into the sand was tracked directly from the image sequences, together with details about pile-up or sinking-in of the sand around the indenter. A continuous record of the indentation force with penetration was obtained using a load cell incorporated into the fixed platen of the testing machine. This enabled a characterization of the resistance of the sand to the indentation, assessment of the ensemble stresses and dissipation and identification of flow characteristics that affect the ensemble force.

IV. ANALYSIS OF THE FLOW FIELD

A hybrid particle tracking technique, used to track fluid flows, was adapted in conjunction with an optical flow algorithm to analyze the image sequences recorded of the indentation region. The purpose was to obtain quantitative characterization of parameters of the flow field, such as velocity, acceleration, strain rate and strain, at high spatial resolution, which are of interest for assessing flow characteristics of the ensemble. The hybrid particle tracking technique combined particle image velocimetry (PIV) and particle tracking velocimetry (PTV) for improved spatial resolution (micrometer-level) of velocity measurement [24], while the optical flow algorithm [22] enabled improved velocity analysis of the non-steady deformation typical of punch indentation. Details of the particle tracking/optical flow and its adaptation to estimate flow parameters are described in the appendix.

The strain rate values of interest to the present study were obtained as

$$\dot{\varepsilon}_{xx} = \frac{\partial u}{\partial x} \text{ where } \dot{\varepsilon}_{xx} \text{ is the component of the strain rate, normal to the axis of the indenter (x-axis)}$$
$$\dot{\varepsilon}_{yy} = \frac{\partial v}{\partial y} \text{where } \dot{\varepsilon}_{yy} \text{ is the component of the strain rate, along the axis of the indenter (y-axis)} \quad (1)$$
$$\dot{\gamma}_{xy} = 2\dot{\varepsilon}_{xy} = \frac{\partial v}{\partial x} + \frac{\partial u}{\partial y} \text{where } \dot{\gamma}_{xy} \text{ is the shear strain rate}$$
$$\dot{\varepsilon}_{eff} = \sqrt{\left[\frac{4}{9}\left(\frac{1}{2}\left(\left(\dot{\varepsilon}_{xx} - \dot{\varepsilon}_{yy}\right)^2 + \dot{\varepsilon}_{xx}^2 + \dot{\varepsilon}_{yy}^2\right) + \frac{3}{4}\dot{\gamma}_{xy}^2\right)\right]}$$

The effective strain rate $\dot{\varepsilon}_{eff}$ a scalar parameter, is often used as a representative quantity for analyzing material deformation; here it is used to elucidate specific aspects of deformation, e.g., flow localization, shear banding, in the granular ensemble.

V. RESULTS

Figure 2 shows an ensemble of 108 consecutive superimposed images of the indentation region. The images were taken from a high-speed image sequence such as seen in the movie (see supplementary material 1). In creating Fig. 2, the background of each of these images was removed and the contrast enhanced so as to make the individual sand particles appear as white features against a dark background in the images. The individual sand particles thus appear to "streak" across the ensemble image as the indentation is carried out. An alternative characterization of Fig. 2 is that it is similar to an image that would have been obtained if the entire experiment was exposed over a single frame. The 'streaks' seen in the image are analogous to path lines in fluid flows.

A. Stagnant zone of material

The most striking feature in Fig. 2 is the presence of a stagnant region of "dead material" attached to the indenter face. The region appears diffuse and somewhat dark in the figure, and is labeled "dead zone";an enlarged picture of this dead zone is shown in the inset to Fig. 2. The geometry of this region in cross-section resembles a curved triangle with two vertices anchored at the edges of the bottom face of the punch. The sides of the triangle meet the punch face at an angle of ~ 27^0. Alternatively, this shape may be described as a circular cap. The material in this zone is essentially stationary with respect to the indenter with no slip occurring at the indenter-zone interface. During indentation, it moves as if it were a rigid block of material attached to the indenter face, indeed acting as an extension of the indenter; this is also clearly seen in the movie (supplementary material 1). The presence of such a dead zone (triangularly shaped) appeared in the slip line field (SLF) solution for plane-strain punch indentation originally proposed by Prandtl, albeit for plastically deforming metals [9]. A similar dead zone under the punch has

been postulated in the SLF forpunch indentation of granular solids,and suggested also by numerical analysis of this problem [25].

The deviation of the pathlines away from the indenter mid-plane in the vicinity of the punch face provides another demarcation of the dead zone (Fig. 2).The pathlines are also clearly symmetric with respect to the mid-plane of the indenter. This is important from an experimental perspective as it shows that the punch is well-aligned, with the load axis perpendicular to the free surface of the sand.

B. Velocity field

The development of the velocity (V) field associated with material flow in the indentation is shown in the movie (supplementary material 2). The velocity vectors are shown superimposed onto velocity magnitudes. This movie is based on image analysis of one of the high-speed image sequences. Eight frames from this movie, spaced 60 seconds apart during the indentation, have been selected (Fig. 3) to describe the development of this field. In analyzing this figure, the supplementary movie and subsequent figures related to flow, the following should be noted. The velocities are normalized with respect to the indenter velocity (V_0), while the half-width (a)of the indenter is used to normalize lengths. With this scaling, the indenter velocity becomes unity. The depth of indentation can also be used as a parameter for characterizing the temporal evolution of the deformation, as time of elapse and depth are equivalent because of the constant velocity of indentation. This depth is recorded along side the time of elapse in Fig.3 in showing the evolution of the deformation field. In Fig. 3 and some of the ensuing figures, the indenter is shown as moving down into the granular ensemble (stationary) rather than as in the experiment where the ensemble is the (upward) moving body. This transformation is done by simply subtracting the velocity of the indentation. This type of presentation or configuration inversion has been done so as to be in conformity with the usual presentation of indentation data.

The velocity field frames in Fig. 3, among other things, enable a characterization of regions of high and low velocity, regions of steep velocity gradients, and the evolution of the field with increasing depth of penetration (or time) of the punch. Irreversible deformation of the granular solid with associated pile-up and lateral displacement of the material in the vicinity of the punch begins quite early on into the indentation process. Likewise, the dead zone (Region 1) is seen to

develop and establish itself quickly even at small indenter penetration (t = 4s; d/a ~ 0.004) extending to a depth (d/a) of about 0.5 units from the bottom face of the punch. The size and shape of this zone, including the characteristic angle of intersection (~ 27^0) of its sides with the punch, change very little during the remainder of the indentation up to t=424s (d/a~0.489). The magnitude and direction of V in the dead zone are essentially the same as those of the punch (Fig. 3), consistent with this zone acting as an extension of the punch and minimal slip along the bottom face of the punch.

A measure of the extent of the deformed region is provided by consideration of where the velocities deviate significantly from zero and/or steep velocity gradients prevail (Fig. 3). This may be done by examining the velocity distribution along different planes in the granular medium as a function of indenter penetration; one such distribution at the indenter mid-plane is shown in Fig. 4. Based on such a characterization, the deformed region is seen to extend to b/a ~3.5 in the horizontal direction and to d/a ~ 1in the vertical direction, at the larger depths of indentation (t = 424s). The evolution of the deformation can thus also be determined from the velocity field sequences (Figs. 3 and 4**)**. Using the mid-plane velocity distribution as a "fingerprint", it is seen from Fig. 4 that the overall deformation settles to a characteristic pattern for t > 124s (d/a~0.143).

A striking feature in the image frames of Fig. 3 is the presence of zones of steep velocity gradients indicative of localized deformation. Several of these are highlighted by dotted lines superimposed onto the frames. These may be thought of as shear bands. The bands demarcate broad regions of relatively uniform velocity, while in themselves they represent local areas of sharp velocity jumps or "velocity discontinuities"; one such shear band is the boundary between the dead zone and the surrounding material. Similar zones of local deformation demarcating broad regions of uniform velocity, albeit of different geometry, have been observed in punch indentation of metals [23].

The evolution of the zones of localized deformation with increasing depth of indenter penetration (or time) is well tracked using the velocity fields (Fig. 3). The deformation pattern (i.e., mobile region) is well established by t = 184s (d/a~0.21), evolving subsequently with little change in its geometric structure, except for local fluctuations in the position of the shear bands and the regions of uniform velocity they demarcate (see supplementary movie 2). If the mid-

plane velocity distribution is used as a "fingerprint" (Fig. 4), then the deformation pattern appears to be well-established for t > 124s (d/a~0.143); that is there is negligible change in the velocity distribution, except for minor fluctuations, at this plane beyond this time. In the early stages of the indentation (t = 64s, d/a~0.073), a region, wherein the velocity is oriented nearly vertically upward, develops close to the indenter edge and extends to the free surface of the sand; this region is labeled as region 2 (Fig. 3). The upward velocity in this region increases with further penetration of the indenter until at t = 124s (d/a~0.143), its magnitude exceeds that of the indenter by ~35%. Material is displaced upward in this region as a consequence of the prevailing velocity field resulting in pile-up of the sand adjacent to the indenter contact with the free surface. With further penetration of the indenter into the sand, this region shrinks somewhat with a greater part of it being subsumed by Region 3. Material flow in Region 3 is characterized by significant components of velocity both in the radially outward and vertically upward directions. This flow contributes to outward (radial) growth of the pile-up region. The evolution of the pile-up with indenter penetration is shown in Fig. 5 as a sequence of line profiles that outline the free surface of the sand at various penetration distances.

C. Rotational flow

An examination of the velocity field in the vicinity of the sharp corner of the punch and side wall reveals another interesting feature of material flow in this granular medium: significant rotational flow or 'vorticity'. This is seen in the movies (supplementary material 1 and 2) and in the image frames of velocity fields in the vicinity of the punch wall shown in Fig. 6. The rotational flow is initiated close to the indenter corner at a small depth of penetration (t = 4s, d/a~0.004). It is strikingly similar to the recirculation zone observed just past a sharp corner in fluid flows. The flow is seen to develop further over a small region adjoining the punch wall, as the depth of indentation increases (this region is demarcated by the thick dotted line in Fig. 6). This "vortex" region is produced as the indenter "drags" sand particles in contact along its wall. The "drag" creates a sharp velocity gradient in the region adjacent to this wall, inducing a "gravitational potential" on the sand surface. This causes sand particles near the surface to the fall into the region immediately adjacent to the indenter wall. At the same time, the bulk motion of the sand flowing past the indenter is in the opposite (upward) direction resulting in this vortex region. The size of the vortex region increases with increasing depth of indentation. Shear

stresses and energy dissipation should be significant in this region as a consequence of the steep velocity gradients and highly rotational flow. It may also be seen from Figs. 5 and 6 that the surface profile of the sand is inclined at ~ 30^0 to the horizontal, which is remarkably close to the angle of repose of ~ 35^0 for this quartzite sand [3]. The optical flow algorithm enables accurate velocity analysis in the vortex region where the flow is highly non-steady, as well as study of development of the sand surface profile.

D. Strain rate

Figure7 shows the effective strain rate field at three different depths of indenter penetration. This field is derived from the velocity field using Eq. (1); high strain rates are synonymous with steep velocity gradients. At small penetration (t = 64s, d/a~0.073), a region of localized high strain rate (~ 0.005/s) is seen at each of the two corners of the punch indicating intense deformation. This localization of deformation, albeit diffuse, is a consequence of concentration of stress at the punch corners and likely also influenced by the rotational flow developing at the corners. With increasing indenter penetration, diffuse shear bands concomitant with local regions of high strain rate are seen to develop across from the tip of the dead zone to the free surface (t = 184s, d/a~0.212; and t = 304s, d/a~0.351). The shear bands are not as sharply defined as those occurring in punch indentation of metals.

VI. DISCUSSION

The deformation field created by a slow moving punch in a granular medium has been studied using image correlation techniques to analyze high-speed image sequences of the flow. The analysis has enabled quantitative characterization of flow and deformation parameters at high resolution, including velocity fields, velocity gradients and strain rate. Based on this characterization, key features of the flow such as dead material zones, path lines, recirculating flows, shear bands and material pile-up have been elucidated. Important insights have been obtained into the development and evolution of this unsteady flow.

The formation of a zone of dead material – dead zone – extending out below the face of the punch, and description of its geometry constitute one key aspect of the current study. While the occurrence such dead zones has been noted in prior studies of granular material flow past obstacles of different shapes [26], the present analysis is notable for elucidating details of the

geometry of the dead zone, and highlighting similarities and contrasts with dead zones occurring in indentation of metals. A dead zone of triangular shape was suggested by Prandtl in 1920 and used in construction of an SLF solution for punch indentation of rigid-perfectly plastic metals [9]. The existence of such a triangular dead zone in metals is clear from Fig. 8,which shows a cap of stagnant material that has developed under the punch when indenting lead, a model rigid-perfectly-plastic metal. The dead zone in sand (Figs. 2 and 3), a curved triangle resembling a circular cap, is markedly different in shape from that of Fig. 8. But theoretical solutions, including of the SLF type, obtained for punch indentation of dilatant granular materials have postulated a triangular dead zone similar to that in metals [25], which is at variance with the experimental observations of the present study. It is well known that geometrical characteristics of the dead zone are strongly influenced by the interface friction condition and indenter shape,in metals. A similar parametric influence on dead zone development may be expected in granular media. The "microscale structure" of the granular media in itself may be of secondary importance to the development of this dead zone, as suggested also by prior observations with different types of particles and beads [26].

Figure 2 shows the sides of the dead zone meeting the punch face at an angle of ~ 27^0, which is a characteristic of this punch-sand interface. Characterization of this angle for different granular material systems or punch-material combinations, should provide direct information about the interface friction boundary condition. However, current theoretical predictions of this angle and dead zone shape are somewhat coarse to enable detailed exploration of the interface friction boundary condition based on dead zone measurements [25] .It may be noted here that assessment of dead zone characteristics based on load-penetration curve for the indentation is generally not feasible because of the relative insensitivity of the load even to the presence or lack thereof of the dead zone [9,25]. This observation holds for both metals and granular media.

The attachment of a stable cap of dead material to the bottom face of the punch results in a change in the indenter shape beyond the very incipient stage of the indentation (t = 4s,d/a~0.004, Fig. 3). Beyond this incipient stage, the dead zone shape and size remain essentially constant. In the present case, the modified indenter shape resembles a circular cap. Furthermore, the observed rapid development of the dead zone suggests that such a zone should also be seen under a fast moving punch or obstacle (including impact loading) and the zone

development should be little influenced by the rate of loading. The evolution of the deformation field beyond the incipient stage is likely to be strongly influenced by the shape of the dead zone. In this context, it is interesting to observe that the two symmetrically located shear bands emanating from the tip of the dead zone (Fig. 3) are similar to those observed under a "finger shaped" indenter with a hemispherical tip [20].

Measurement of the velocity field at high resolution has enabled, among other things, characterization of regions of steep velocity gradients (Figs. 3, 4 and 6) and of the strain rate tensor. While details of the strain rate tensor have not been presented here, the scalar effective strain rate has been estimated from the strain rate tensor (Fig. 7). The effective strain rate and the velocity field are the representative parameters used to describe the deformation of the granular ensemble. The strain rate (not strain) field captures the local deformation best since it is a measure of the incremental strain imposed per unit time. This field can also be viewed as the analog of the plastic failure mechanism usually alluded to in case of deformation of elastic-plastic metals [8, 26]. Analysis of the velocity and strain rate fields has shown that the deformation and flow reach a "state of equilibration", even for this geometry of unsteady deformation, within the relatively small penetrations studied. This state is characterized by a stable dead zone of defined shape anchored to the punch face, a characteristic deformation and shear band pattern, and flow zones adjoining the punch walls with significant recirculation and vorticity (Figs.3 and 6, $t > 124$s, $d/a > 0.143$). The velocity field for this state shows broad similarity with the well known Prandtl's slip line field [9, 25] except for differences in the specific shapes of the deformation zones such as the dead zone. Also, the SLF does not postulate a region of rotational flow adjoining the punch walls.

While forces were measured as a function of penetration of the punch into the sand, correlations between deformation and stress fields were not explored. This type of correlation has important implications for understanding flow behavior of granular solids, much more so than in metals. In classical metal plasticity, the deformation field generally coincides or is strongly correlated with the stress field via an associated flow rule. In contrast, with granular media, the kinematic and static fields need to be investigated independently because of substantial non-associativity in the flow rules. Deformation measurements of the type presented in this study offer a means for

exploring flow rules in granular solids, by studying the relation between force chains and the deformation field; this is envisaged in the near future.

Pile-up of sand in the vicinity of the punch has been observed and characterized (Fig. 5). The geometric characteristics of the pile-up region show important similarities with that observed in punch indentation of highly strain-hardened metals [9]. The highest point in the pile-up region is seen to be located at some distance from edge of the indentation (b/a ~ 2.5), likely due to the development of the region of rotational flow along the walls of the indenter. The evolution of the pile-up including the location of the peak is consistent with the flow pattern observed in the material: lateral outward displacement of the material in Region 3 is coupled with the upward displacement in Region 2 resulting in the pile-up (Fig. 3, t = 124s, d/a ~ 0.143). The observations based on continuous tracking of the sand motions and velocities suggest that the pile-up is likely influenced by the sand characteristics and hydrostatic pressure. Furthermore, the repose in the sand allows the grains to roll over and retain contact with the indenter unlike what has been observed in metals, compare and contrast Figs. 2 and 8 [23]. This rolling over of the grains plays an important part also in the development of the vortex structures adjoining the punch walls (Fig. 6).

Measurements in the vortex region, indicate that the angular velocities are large, and dissipative forces are likely significant. The dissipation mostly arises from the friction between the sand particles and will result in a drag analogous to "form drag" observed in fluid flow past a sharp obstacle. This type of rotational flow has not been observed in punch indentation of metals. It may be possible to eliminate or modulate this region drawing from fluid notions such as streamlining the corner of the punch, for example by incorporating a small radius. More detailed measurements of this rotational flow and dissipation should be of value for understanding motion of objects such as reptiles and robots through sand [7].

In summary, the high-resolution measurements have provided detailed quantitative information of deformation and flow of a granular ensemble past a slow moving, flat punch indenter. While this information is in itself of value for validating and/or discriminating between theories of flow, exploration of flow rules for granular ensembles, and understanding of friction in granular solids, the importance of the results for applications cannot beoverlooked. The deformation field in punch indentation has important implications for processing of granular solids and powder

particulate into bulk forms by methods such as rolling, compression forging and extrusion. For example, the shape and dimensions of the dead zone will influence the minimum size of sheet and foil that can created by consolidation, including in processing of pre-forms and tablets in the pharmaceutical sector. The inhomogeneity in the deformation field such as arising from shear bands and dead zones will impact defect generation in processing, as well as uniformity of properties of the resulting consolidate. The forces required for processing of the granular solids, and drag encountered by objectswhen moving through sand will be determined by the flow and dissipation. These aspects of flow and deformation processing, and their relation to punch indentation are well established for metals;such understanding has resulted in improved bulk deformation processing of metals [5, 9]. Quantitative studies of indentation such as presented in this study should enable similar development of the theory of flow and deformation processing of granular solids.

VII. CONCLUSION

The deformation field created by a slow moving punch in a granular medium has been studied using image correlation techniques applied to high-speed image sequences of the flow. The analysis has enabled quantitative characterization of flow and deformation parameters at high resolution, including velocity fields, velocity gradients and strain rate. Based on this characterization, key features of the flow such as dead material zones, path lines, highly rotational flow and vortices, shear bands and material pile-up have been elucidated. Important insights have been obtained into the development and evolution of this unsteady flow. The results provide quantitative data for refinement of theoretical models of flow of granular ensembles. Future experiments will explore the role of friction at the indenter-punch interface, and its implications for dead zone and vortex formation.

ACKNOWLEDGEMENT

T.M would like to acknowledge support of the Department of Science and Technology, Govt. of India for financial support. S.C would like to acknowledge NSF grants CMMI 1100712 and

0928337 for partial support of this work. We would like to thank Dr. Narayan Sundaram of Purdue University for his comments on the manuscript.

1. F. Radjai, D.E. Wolf, M. Jean and J.J.Moreau, Phys. Rev. Lett. **80**,61 (1998).
2. M.R. Kuhn, Granular Matter **4**, 155 (2003).
3. J. Duran, *Sands, Powders, and Grains* (Springer-Verlag, New York, 2000).
4. F.V. Lenel, *Powder Metallurgy: Principles and Applications* (Metal Powder Industries Federation, 1980).
5. W. A. Backofen, *Deformation Processing* (Addison-Wesley Pub. Co., USA, 1972).
6. J. Litster and B. Ennis, *The Science and Engineering of Granulation Processes* (Kluwer Academic Publishers, USA, 2004).
7. Y.Ding, N. Gravish and D.I. Goldman, Phys. Rev. Lett. **106**, 028001 (2011).
8. K.Terzaghi,*Theoretical Soil Mechanics* (John Wiley and Co., USA 1966).
9. R. Hill,*The Mathematical Theory of Plasticity* (Oxford University Press, Oxford, 1950).
10. T. S. Majumdar and R.P. Behringer, Nature, **435**, 1079 (2005).
11. B. Utter and R.P. Behringer, Phys. Rev. Lett., **100**, 208302 (2008).
12. P. Schall and M. van Hecke, Ann. Rev. Fluid. Mech., **42**, 67 (2010)
13. M. Muthuswamy and A. Tordesillas, J. Stat. Mech., **09003** (2006).
14. N.P. Kruyt and S.J. Antony, Phys. Rev. E, **75**, 051308 (2007).
15. A. Drescher, Geotechnique, **26**, 591 (1976).
16. W. Sylwestrowicz, J. Mech. Phys. Solids, **1**, 258 (1953).
17. D.J.White, W.A. Take and M.D. Bolton, Geotechnique, **53**,619 (2003).
18. D.J.White and M.D. Bolton, Geotechnique, **54**, 375 (2004).
19. T.G. Murthy, E. P. Gnanamanickam, C. Saldana and S. Chandrasekar, AIP Conf. Proc., **1145**, 263 (2009).
20. E. Hamm, F. Tapia and F. Melo, Phys. Rev. E, **84**, 041304 (2011).
21. M. Erpelding, A. Amon and J. Crassous, Phys. Rev. E, **78**, 046104 (2008).
22. T. Liu and L. Shen, J. Fluid Mech., **614**, 253 (2008).
23. T. G. Murthy, C.Huang and S.Chandrasekar, J. Phys. D: Appl. Phys., **41**, 074026 (2008).

24. E.P. Gnanamanickam, S. Lee, J.P. Sullivan and S. Chandrasekar, Meas. Science and Technol., **20**, 095710 (2009).
25. A. Tordesillas and J.Shi, Proc. Roy. Soc. A, **455**, 1981,261 (1999).
26. Y.Amarouchene, J.F. Boudet and H.Kellay, Phys. Rev. Lett. **86**, 4286 (2001).
27. J. Lubliner, *Plasticity Theory* (Dover, USA, 2008).
28. T. Corpetti, D. Heitz, G. Arroyo, E. Memin, A. Santa-Cruz, Exps. Fluids, **40**, 80 (2006).
29. I. Christadler, H. Köstler, U. Rüde, In Proceedings of 18th Symposium Simulations Technique ASIM (2005).

APPENDIX:IMAGE ANALYSIS

The background and details of the image analysis techniques used to analyze the flow are discussed in this section.

In fluid mechanics, the goal of most tracking measurements is to obtain full flow (velocity) fields by tracking particles or particle agglomerates. These particles may be intrinsically present in the flow ordeliberately injected into it. Continuous images of the flow are then acquired at a frame rate dictated by the time scale of the problem under study. A computer vision algorithm in this application thus, includes a pattern recognition subroutine to identify individual particles or groups of particles and a subroutine to track these particles/features between two subsequent images. Such techniques are loosely referred to as particle tracking velocimetry (PTV) techniques. A subfield of PTV is particle image velocimetry (PIV), which in its most basic form involves injecting tracers or particles into the fluid and tracking the motion of ensembles of these particles by digitizing images of the flow. The digitized images are divided into windows called interrogation windows. Each window is cross-correlated with a corresponding window in a subsequent image to calculate the particle displacement field and the velocity field. The location of the peak of the cross-correlation function is a direct measure of the average displacement of the particles within an interrogation window.

General PTV techniques are higher order extensions of PIV, in which individual particles within an interrogation window are tracked, usually to improve the estimation of velocities. The present

study employs one of these PTV techniques - a hybrid PIV/PTV technique – for the flow field mapping based on resolution considerations. Typically, these hybrid techniquesuse correlation-based PIV to first obtain an ``estimate'' of the velocity vectors in a fairly coarse interrogation window. This estimate is then used to calculate displacements of individual particles within that window using a PTV technique, often enabling velocity measurements at the micrometer-scale. PIV/PTV techniques have been adapted to study various flow fields including micron-scale fluid flows at high (micrometer-scale) resolution. The hybrid PIV/PTV method used here was originally developed to study large strain deformation in metals arising from indentation and material removal [24].

The advantage of a hybrid PIV/PTV technique over pure PIV is enhanced spatial accuracy (~$1/10^{th}$ of a pixel) of velocity estimation. However, while carrying out instantaneous measurements of velocity fields in an unsteady deformation process, such as punch indentation, the PIV/PTV system has some drawbacks. Chief among these is that the distribution and the density of velocity vectors are dependent on the particle distribution. The higher the density of particles that are available for tracking, the higher is the density of velocity vectors obtained in the flow field. One “particle” in a PTV system yields only one velocity vector. Animage analysis technique used to overcome this deficiency is called optical flow. Liu and Shen [22] define optical flow as “*the velocity field in the image plane that transforms one image into the next image in a time sequence*”. Mathematically, it defines the velocity field that maps the intensity distribution of one image with that of a subsequent image subject to some assumptions. The optical flow technique as applied to particle/feature tracking in fluid flows has been reviewed in detail by Liu and Shen [22] and Corpetti et al. [28]. This optical flow method can be used to obtain instantaneous high-resolution velocity field measurements from a sequence of images. Ideally a continuously varying flow field such as in indentation of sand will yield one velocity vector per pixel. Quantitatively, PIV/PTV uses the center of a particle to estimate its motion while optical flow tracks the entire particle itself to yield its displacement. Hence, every pixel yields a velocity vector as long as the pixel is illuminated by some portion of a particle.

An optical flow algorithm was used in conjunction with the aforementioned hybrid PIV/PTV to estimate velocity fields in the present study. This flow algorithm is that used by Liu and Shen

[22]. A brief description of the technique is presented. Liu and Shen [23] have derived a physics-based optical flow equation

$$\frac{\partial I}{\partial t} + \nabla \cdot (I\vec{u}) = f(x, y, I)$$

where, I, is the intensity of a given pixel, $\vec{u}$, the velocity vector at that pixel. *f(x,y,I)*is a function that is dependent on the particular particle visualization technique. To determine the optical flow ($\vec{u}$) a smoothness constraint is added to this optical flow equation and a function,

$$J(\vec{u}) = \int_A \left[\frac{\partial I}{\partial t} + \nabla \cdot (I\vec{u}) - f \right]^2 dxdy + \alpha \int_A \left[|\nabla u|^2 + |\nabla v|^2 \right] dxdy$$

is defined, where, α is the Lagrange multiplier. $J(\vec{u})$, is minimized using standard optimization techniques yielding the corresponding Euler-Lagrange equation,

$$I\nabla \left[\frac{\partial I}{\partial t} + \nabla \cdot (I\vec{u}) - f \right] + \alpha \nabla^2 \vec{u} = 0$$

This Euler-Lagrange equation is then discretized and solved for, using a Jacobi's block-wise iteration technique to yield a velocity vector for each pixel. The solution obtained from the hybrid PIV/PTV technique is used as an initial estimate of the velocity field for the optical flow techniques so as to obtain faster convergence.

The direct outputs of the aforementioned image analysis are velocity (vector) fields from which other flow field parameters such as strain rates, incremental strains and dilatation can be estimated. In the present study, the Lagrange multiplier was chosen as 5000. To preserve edges, an edge detection routine was coupled with the optical flow algorithm that set the Lagrange multiplier to zero at edges to minimize smoothing across edgessimilar to the isotropic Lagrange multiplier suggested by Christadler et al [29]. This was done across the indenter face and the surface profile of the sand as the indentation proceeded.A similar edge detection algorithm was used to estimate the time evolution of the sand surface profile. At the boundaries (both the indenter and the surface profile of the sand), the velocities at the boundary were set to the

average velocity of the neighboring pixels interior to the flow field. The images were pre-processedwith a Gaussian smoothing filter of radius 35 pixels and standard deviation of 20 pixels to obtain a smooth intensity distribution across the image.

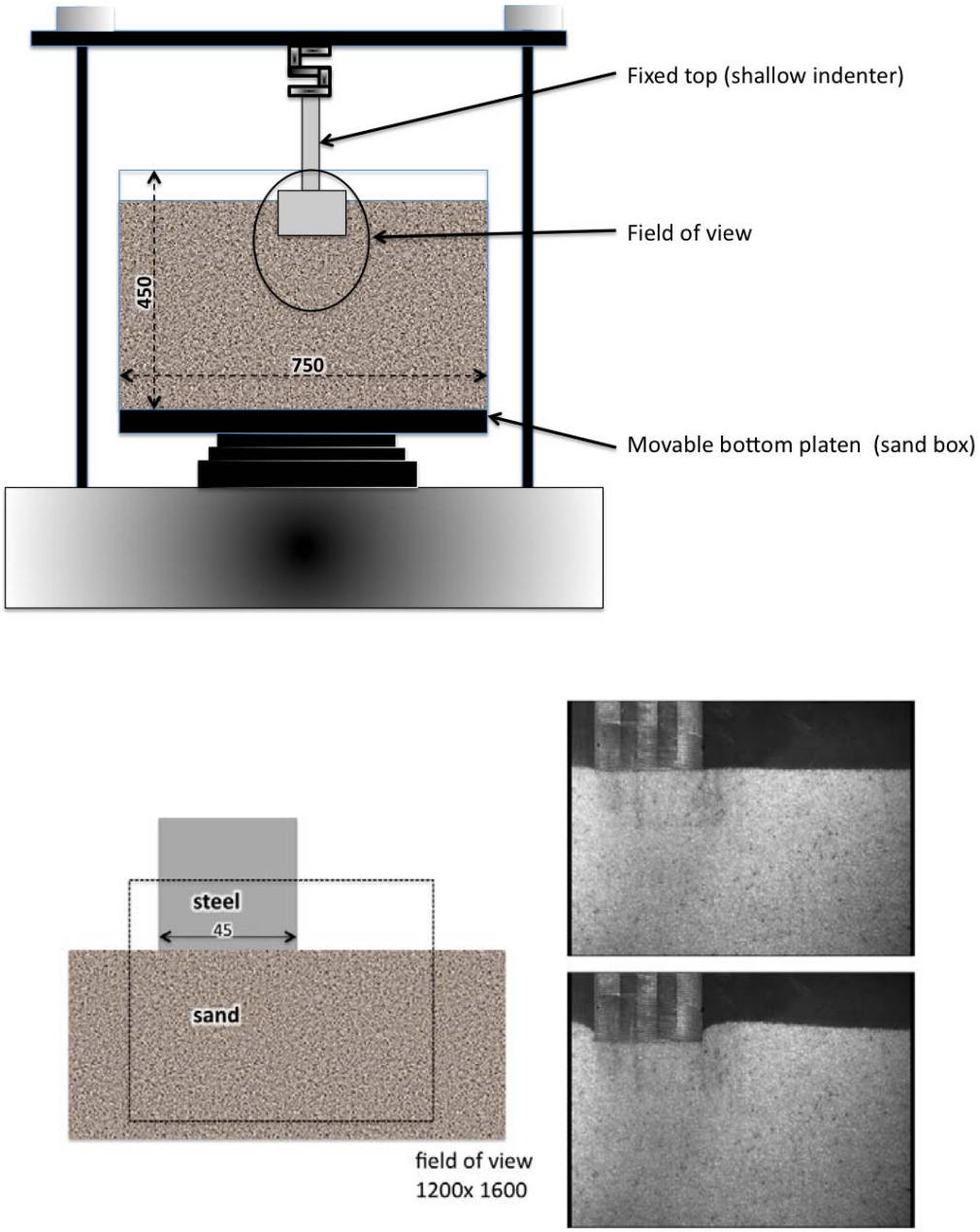

FIG.1 Schematic of the experimental set-up. The indenter is attached to the fixed crosshead of a UTM while the sand is contained in a Perspex chamber placed on the moving machine base. The velocity of indentation (V_0) was set at 0.016mm/s. The field of view, fixed with respect to the indenter and imaged during the indentation, is highlighted. The image size was 1200x1600 pixels. Two sample images at different stages of the indentation are shown. All dimensions are in mm.

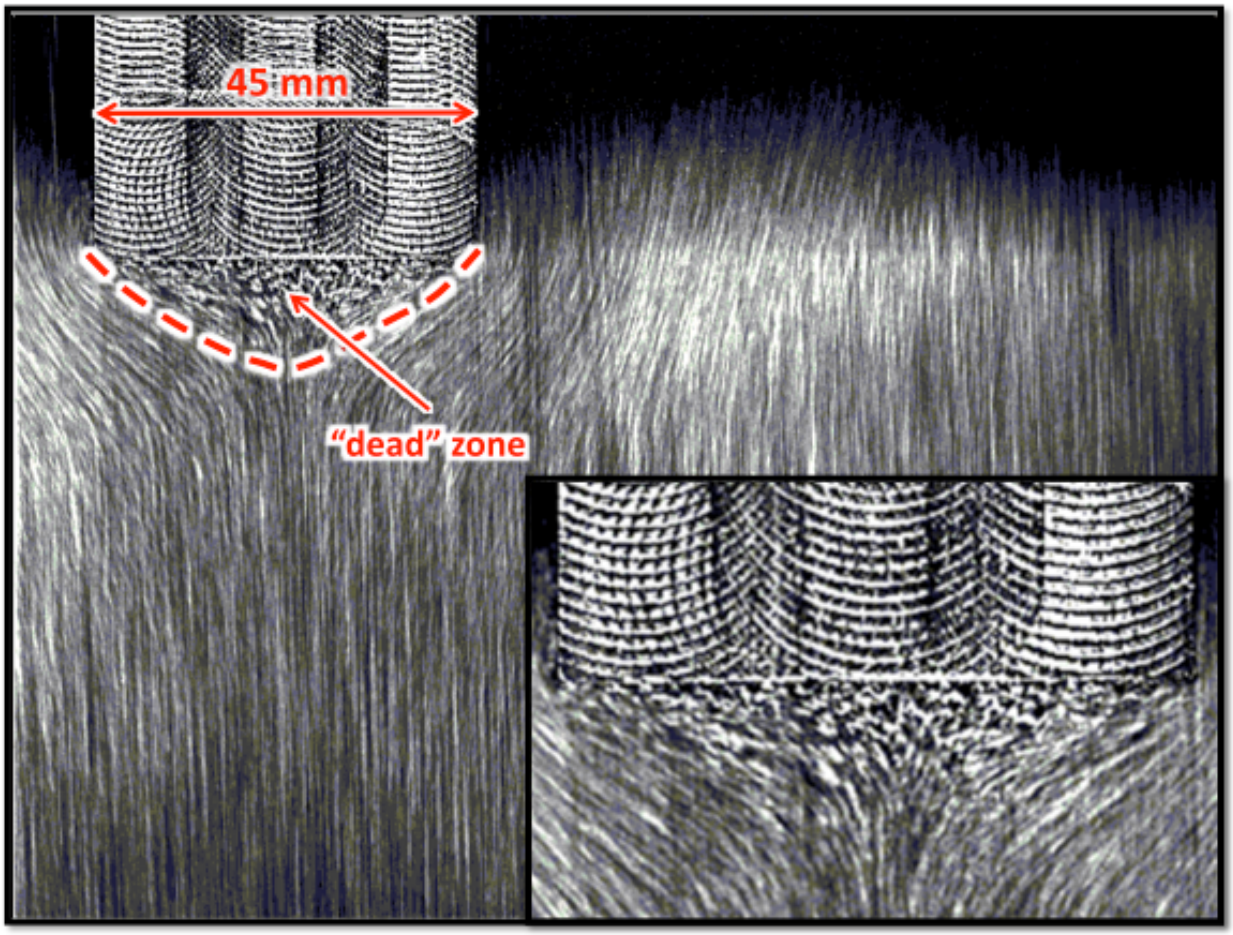

FIG. 2 Ensemble composed by superimposition of 108 consecutive images of the indentation region.The 'streaks' are the analog of pathlines in fluid flows. The inset shows a magnified view of the region of stagnant material - the "dead zone".

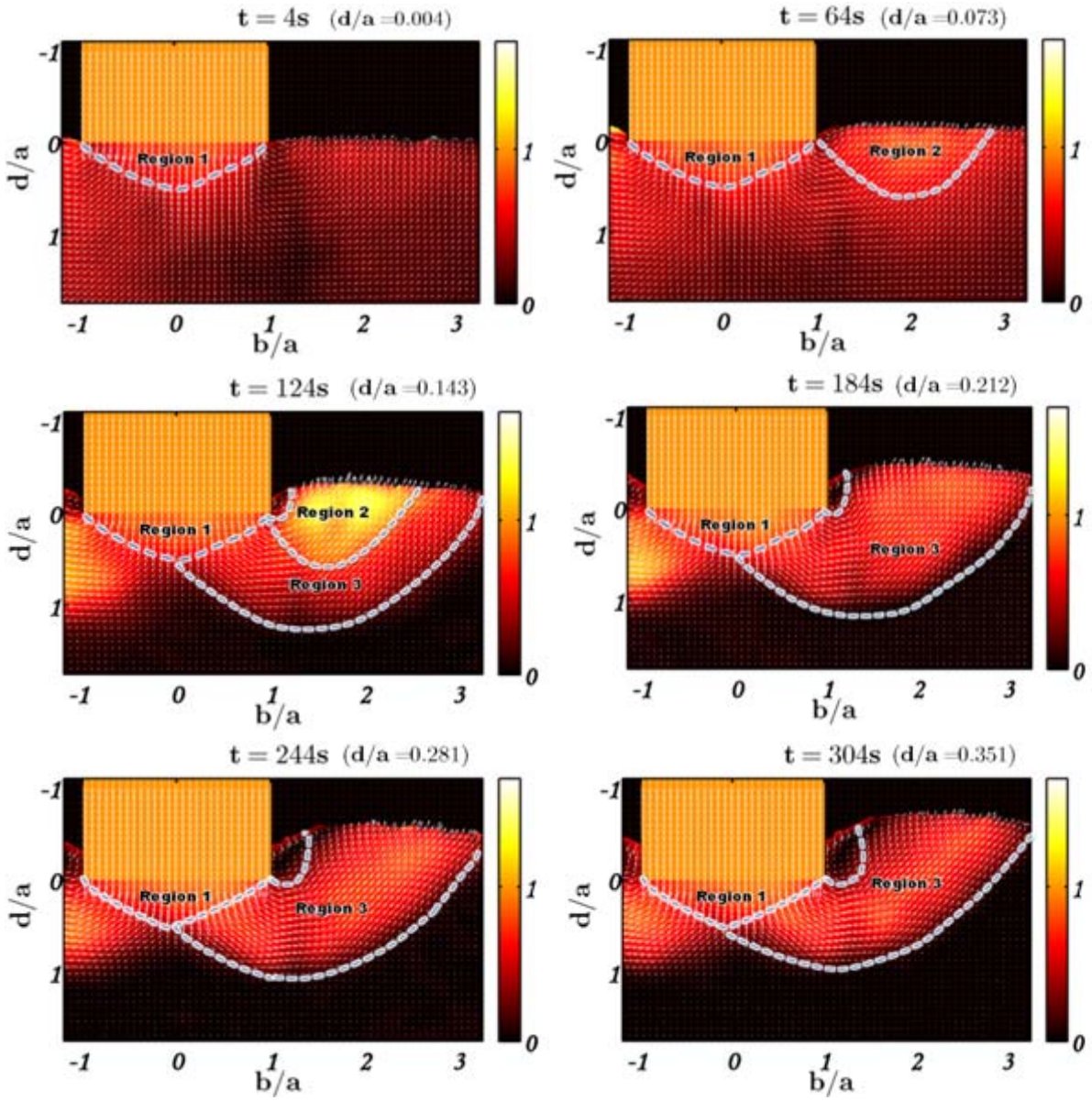
t = 4s (d/a =0.004)
t = 64s (d/a =0.073)
t = 124s (d/a =0.143)
t = 184s (d/a =0.212)
t = 244s (d/a =0.281)
t = 304s (d/a =0.351)
Region 1
Region 2
Region 3
d/a
b/a
-1
0
1
2
3

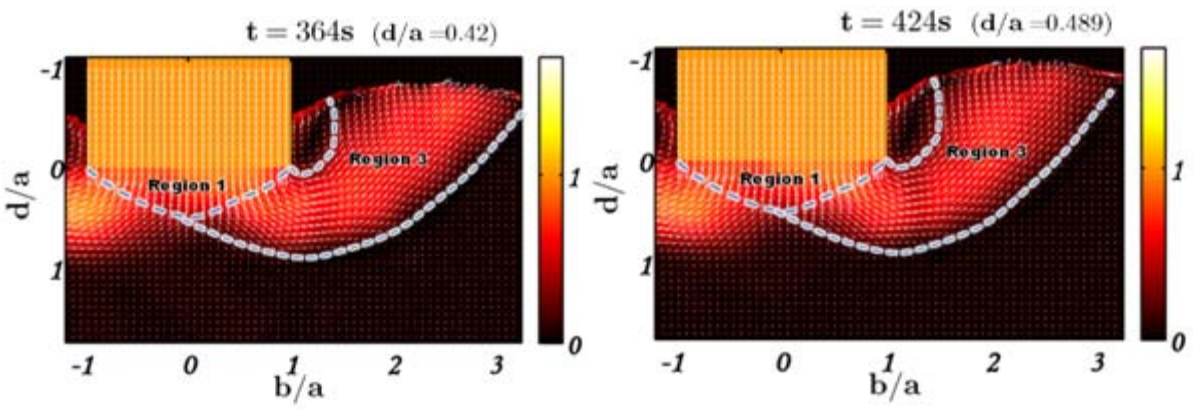

FIG. 3 Evolution of velocity (V/V_0) field with increase in indentation depth. The field shows a distinct 'dead zone' (Region 1) that remains essentially constant throughout the indentation. Regions 2 and 3 show variation in both magnitude and extent with indentation (t >124s), with Region 2 eventually being mostly subsumed within Region 3.

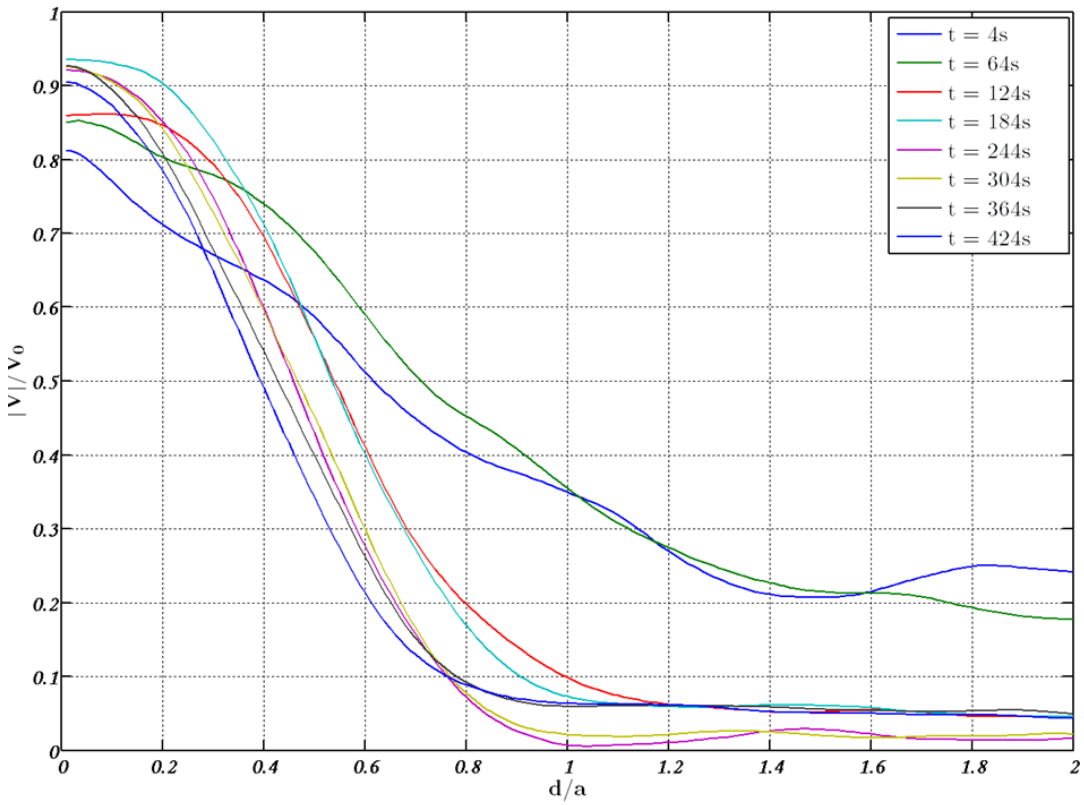

FIG.4 Velocity distribution along the mid-plane of the indenter, as a function of indenter penetration (time). The deformed region is seen to extend to d/a ~ 1 in the vertical direction, at the larger penetrations of the indenter (t = 424s).

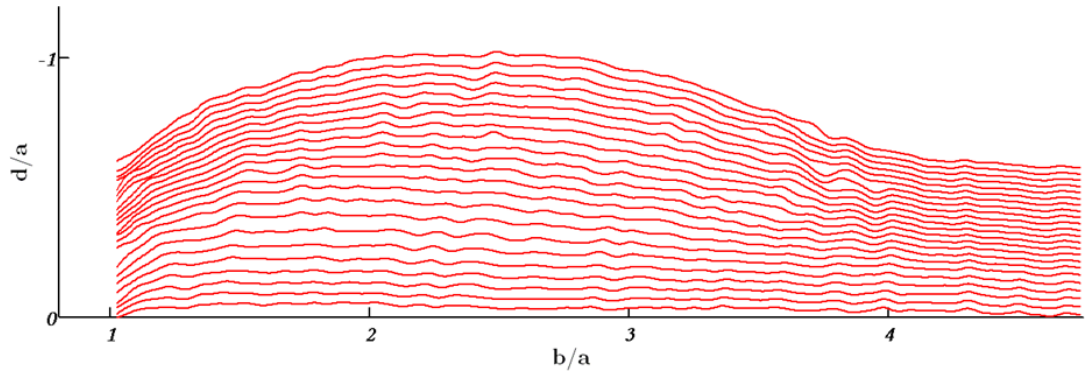

FIG. 5 Evolution of profile of the free surface of sand with increasing depth of indentation. The pile up of the sand shows a maximum at distance b/a ~ 2.5 from the center line of the indenter.

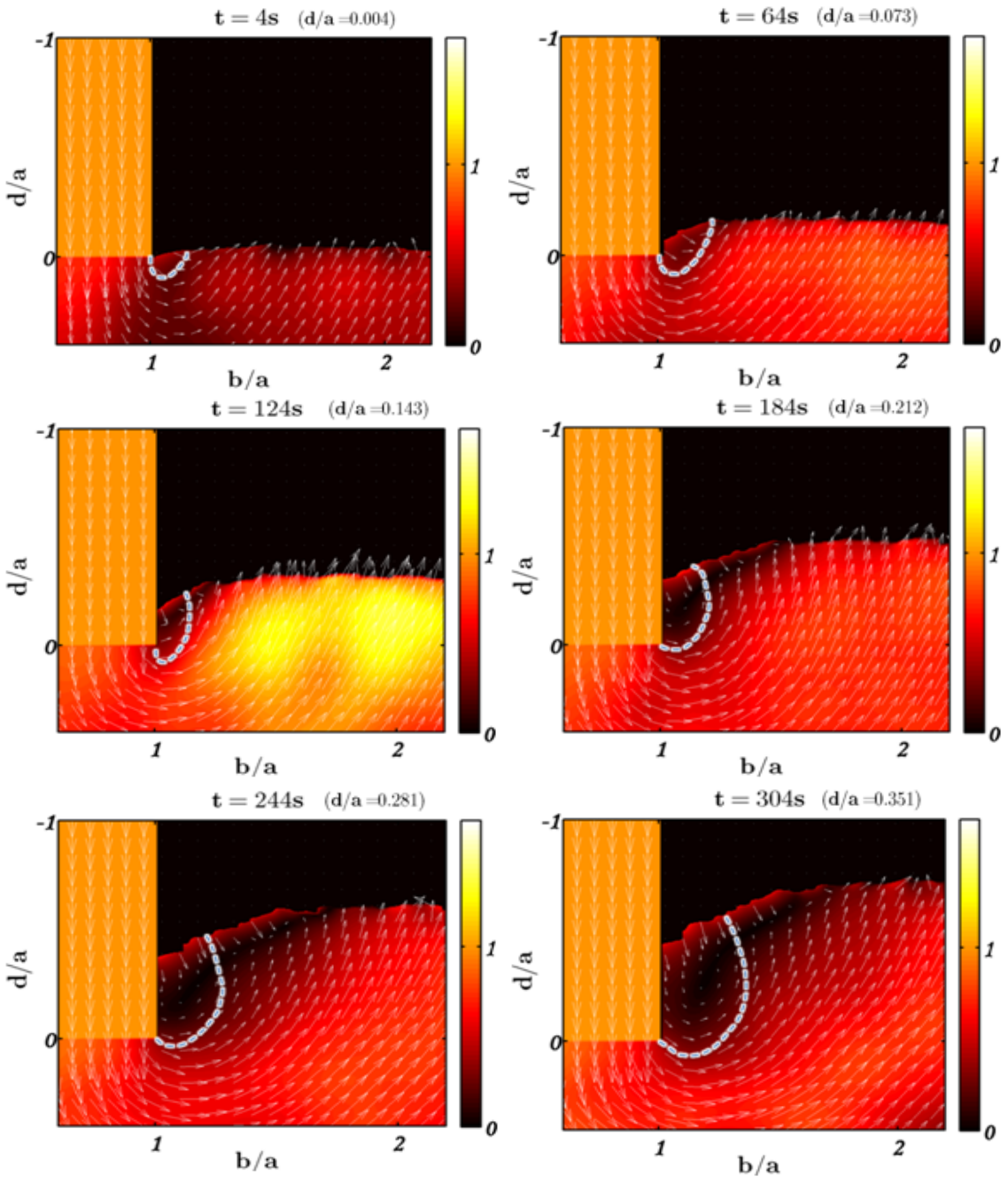
t = 4s (d/a =0.004)
t = 64s (d/a =0.073)
t = 124s (d/a =0.143)
t = 184s (d/a =0.212)
t = 244s (d/a =0.281)
t = 304s (d/a =0.351)
d/a
b/a
-1
0
1
2
1
0

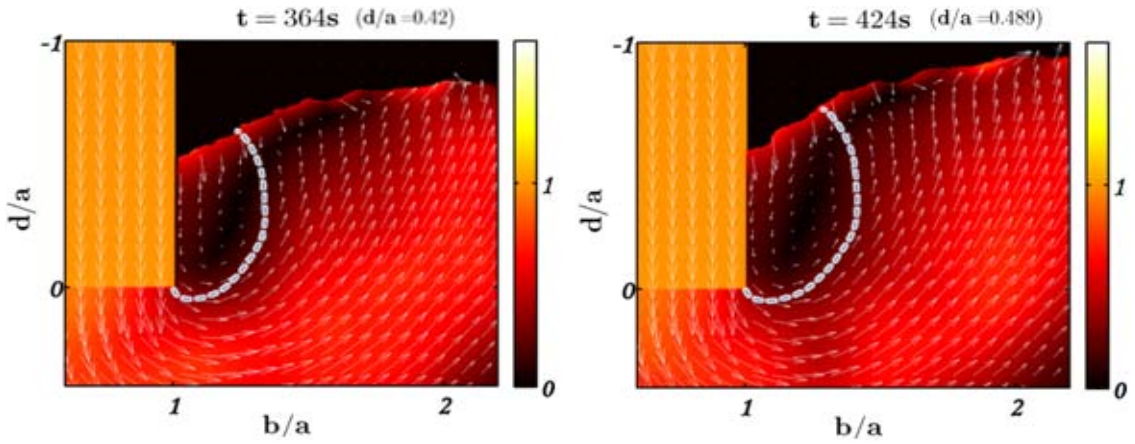

FIG. 6 Velocity field in the vicinity of the corner of the punch and side wall showing highly rotational flow or vorticity. This vortex region is demarcated by a thick dotted line and may also be seen in the movies (supplementary material 1 and 2).

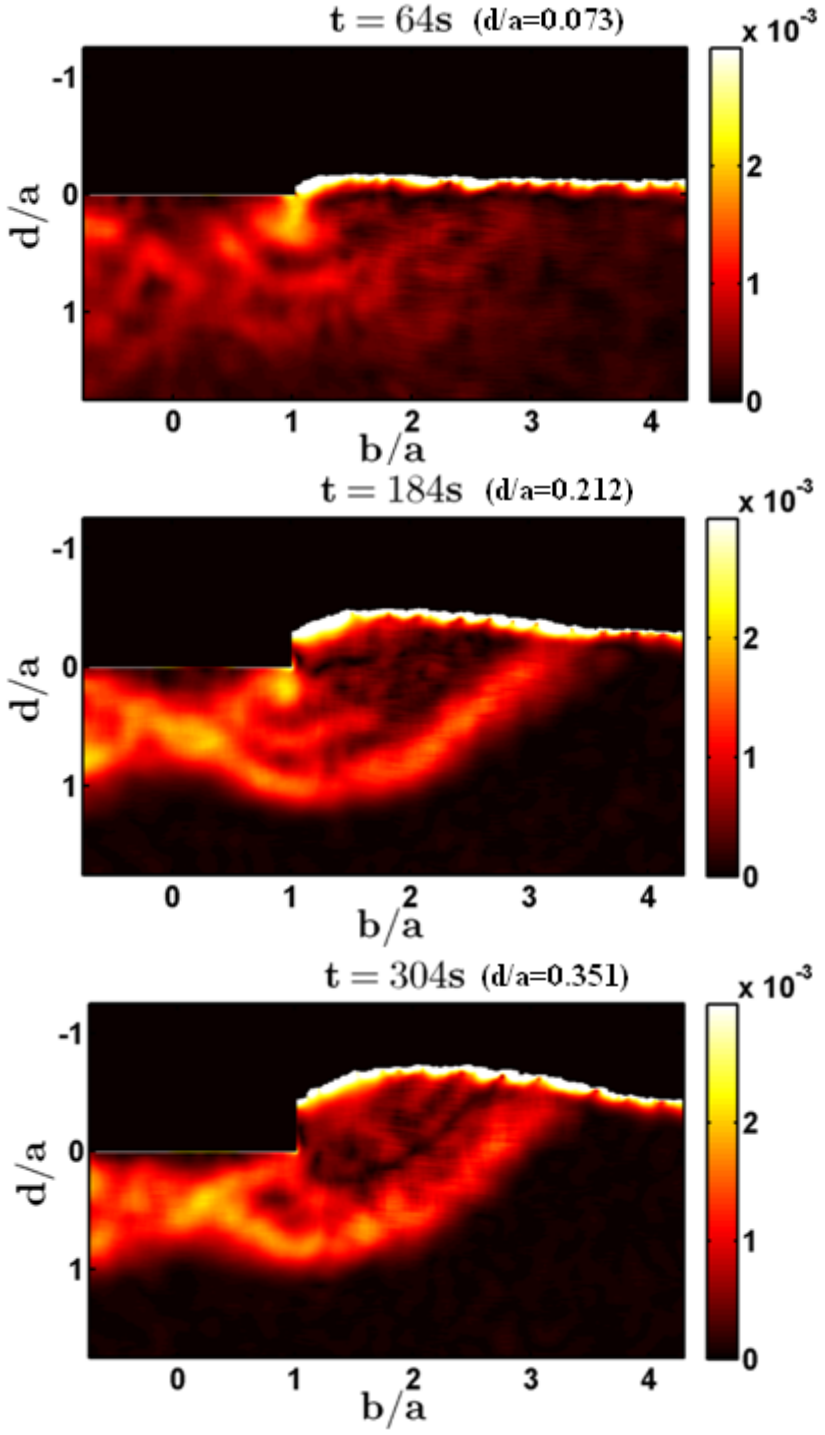

FIG.7 Evolution of effective strain rate with increasing depth of indentation. The effective strain rate is a scalar signifying, among other things, the magnitude of jump or change in the velocity.

The regions of high strain rate may also be thought of as shear bands developing in the granular ensemble. The strain rate has units of sec^{-1}.

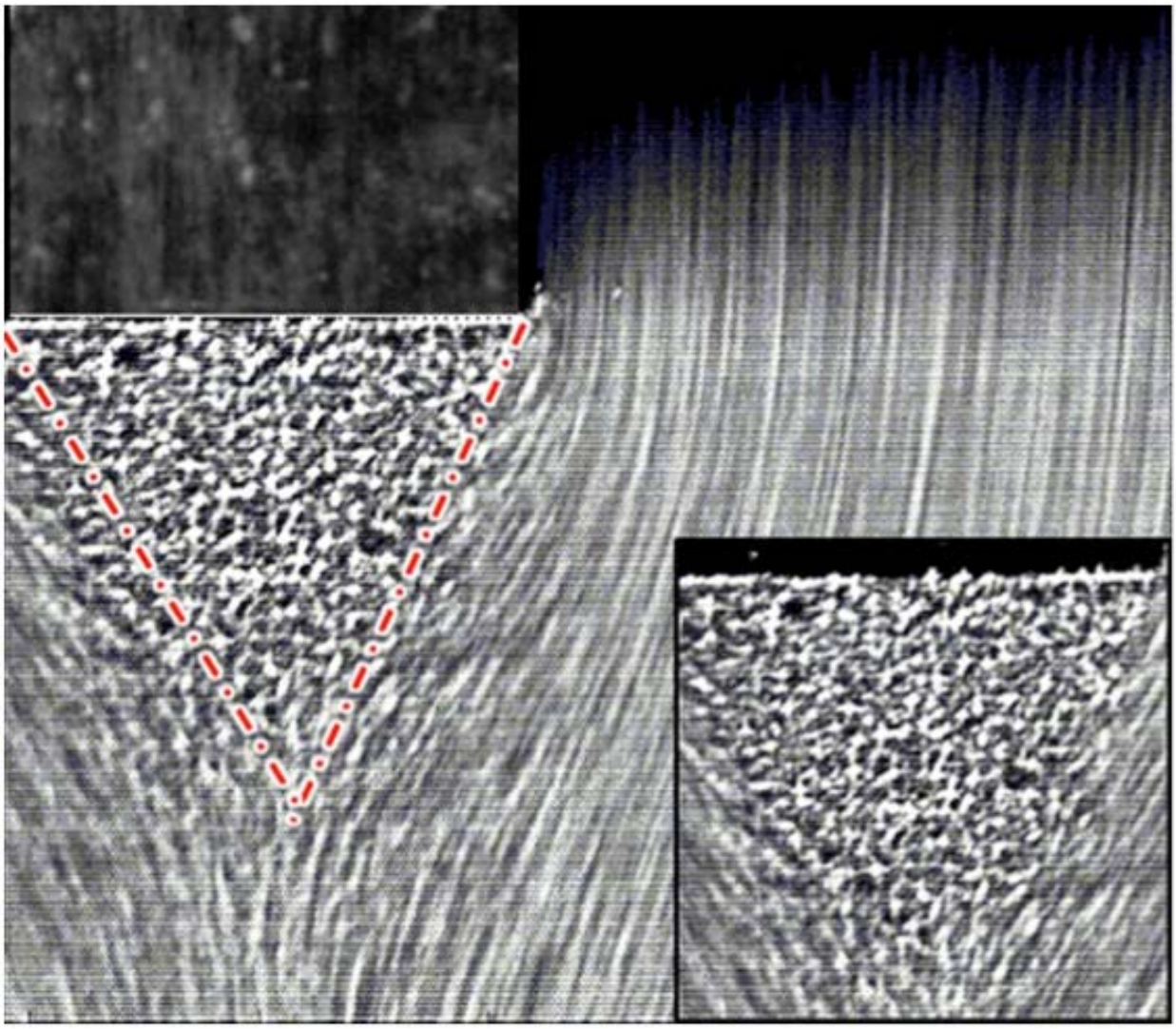

FIG. 8 An ensemble of 80 consecutive images in indentation of lead showing triangular dead zone geometry. The asperities present on the side face of the lead under observation appear as ‘streaks’ in the image, analogous to the streaking sand particles. Note also the small gap

between the indenter wall and the metal in contrast to the vortex region present herein in sand indentation